Seismic, Shock, and Vibration Isolation

1990

PVP - Vol. 200

Seismic, Shock, and Vibration Isolation — 1990

presented at

THE 1990 PRESSURE VESSELS AND PIPING CONFERENCE
NASHVILLE, TENNESSEE
JUNE 17–21, 1990

sponsored by

THE PRESSURE VESSELS AND PIPING DIVISION, ASME

edited by

H. H. CHUNG
ARGONNE NATIONAL LABORATORY

THE AMERICAN SOCIETY OF MECHANICAL ENGINEERS
United Engineering Center • 345 East 47th Street • New York, N.Y. 10017

ISBN No. 0-7918-0513-1

Library of Congress
Catalog Number 88-71319

FOREWORD

The subject of seismic, shock, and vibration isolation of structures and equipment continues to draw much interest and attention in the building and nuclear industries.

Since 1987, the ASME Pressure Vessels and Piping Division has been successfully sponsoring the Symposium on Seismic, Shock, and Vibration Isolation. This year's publication contains seven papers presented at the Fourth Symposium in this series at the 1990 ASME Pressure Vessels and Piping Conference, Nashville, Tennessee, June 17–21. The symposium consisted of three paper sessions in which eleven papers were presented, and one panel session in which the design and manufacturing aspects of seismic isolation were discussed. Four papers were not published here as they report the progress of current R&D efforts.

One of the most important aspects of vibration isolation is to protect the secondary structure (e.g., equipment) contained in the primary structure (e.g., building) subjected to vibratory motion such as an earthquake. Fan and Ahmadi studied base-isolated buildings and brought much insight to the subject. The effects of equipment/building interactions and the comparison of various isolation systems are studied. The authors conclude that the laminated rubber bearing system is most effective in minimizing the equipment response.

Tajirian, Kelly, Aiken, and Veljovich propose a 3-D seismic isolation system capable of accommodating horizontal and vertical ground motions for buildings with low aspect-ratio. Through an extensive test program, the feasibility of the 3-D isolator was demonstrated and future R&D efforts are identified.

The paper by Wu and Seidensticker presents the in-situ test results and the actual performance information of a seismically isolated building subjected to a recent earthquake in Japan. The authors also performed an analytical verification study to evaluate the performance data.

Shiojiri and Ishida discuss some results of seismic isolation study at the Central Research Institute of the Electric Power Industry (CRIEPI) in Japan. Scale-model tests of laminated elastomers with lead-plug and a combination of laminated elastomers and viscous dampers were performed as an important step toward the application for Japanese Liquid Metal Reactors (LMR).

The paper by Bonacina, Torda, Giuliani, Forni, Martelli, Masoni, and Spadoni provides an overview of an Italian R&D program on seismic isolation. The authors discuss some interim results and the need for codes and standards, international collaboration, and future R&D efforts.

In the paper by Nicholson, the design of the exposed surface of elastomeric bearings is discussed. Analytical study was performed to address the stress singularities associated with the "wedge problem."

Finally, Revesz and Hueffmann discuss the advantages of using viscous dampers in lieu of mechanical snubbers for piping system support. They also present an analytical method for designing viscous dampers.

The work reported here is representative of current R&D activities and design studies. The editor hopes this volume will serve as a useful resource for the interested engineers in seismic, shock, and vibration isolation area.

The editor wishes to express his gratitude to the authors for their contribution to this volume and to the reviewers for their conscientious and constructive criticism.

Howard Chung
Argonne National Laboratory
Argonne, Illinois

CONTENTS

RESPONSES OF EQUIPMENT IN BASE-ISOLATED STRUCTURES UNDER EARTHQUAKE GROUND MOTIONS

F.-G. Fan and G. Ahmadi
Department of Mechanical and Aeronautical Engineering
Clarkson University
Potsdam, New York

ABSTRACT

Numerical simulations of seismic responses of equipment in base-isolated structures are considered. A three-story building is used as the primary structure, while the equipment is modeled as a single-degree-of-freedom linear system. The interactions between the the equipment and the structure are included. A number of base isolation systems such as the Laminated Rubber Bearing, the Pure Friction, the Resilient-Friction, and the Electricite de France systems are considered. The N00W component of El Centro 1940 earthquake accelerogram is used as the ground excitation. Acceleration response spectra of the equipment under different conditions are evaluated and the effects of equipment-structure interactions are studied. It is shown that the use of base isolation provides considerable protection for structural contents. However, the peak responses of the equipment vary substantially depending on the base isolation systems used. Among the base isolation systems considered, the Laminated Rubber Bearing system appears to be remarkably effective in reducing the peak responses of equipment under a variety of conditions.

INTRODUCTION

The goal of aseismic design is to protect the structure, as well as the structural content. During an earthquake, a fixed-base shear frame structure filters the generally broad-band ground excitation into narrow-band responses at various elevations. The equipment contained in the structure are then excited by these floor motions and interact with the primary structure. Due to tuning or near tuning, certain secondary systems may be damaged significantly even in a low intensity earthquake. There have been numerous examples that non-structural components experienced major damages while the structure itself survived the earthquake attack. In earthquake resisting design of structures containing critical and/or expensive equipment such as nuclear power plants, hospitals, computer centers, and telecommunication buildings, protection of secondary systems is as important as the structure itself.

In contrast to the conventional strengthening methodology, an alternative aseismic design strategy is to isolate the structure from the ground excitations during earthquakes. In the past two decades, several base isolation systems for stiff and compact structures were proposed, and their performances were studied. Kelly [1,2] provided extensive reviews on earlier and recent developments on the subject. Numerous reported numerical simulations and shaking table experiments have shown that the peak transmitted accelerations and the deflections generated in the structures are dramatically reduced by using properly designed base isolation systems [1,2]. However, consequences of use of various base isolation devices on responses of secondary systems are not fully understood. In particular, the presence of frictional elements in a base isolator may have adverse effects on certain secondary and non-structural components. Recent studies of Su et al. [3] and Fan et al. [4,5] showed that high frequency components are generated in the acceleration responses of a structure with a frictional base isolation system. These high frequency motion could be damaging to stiff equipments and non-structural attachments.

Numerous theoretical, numerical, and experimental studies on responses of secondary systems in fixed-base structures have been performed [6-11]. A state-of-the-art review on response analysis of secondary systems was recently provided by Chen and Soong [12]. On the other hand, studies on secondary system responses for base-isolated structures are rather scarce. Some experimental and theoretical results were provided in [13-16]. Recently, Fan and Ahmadi [17] conducted a comparative study of the floor response spectra for a multi-story building with various frictional and rubber bearing type base isolation devices. It was shown that the features of these floor spectra vary significantly depending on the type of base isolation systems used.

In this work, seismic responses of secondary systems in base-isolated structures under various earthquake ground excitations are studied. The interactions between the secondary system and the primary structure are included in the analysis. Several base isolation systems including the Laminated Rubber Bear-

ing, the Pure Friction, the Resilient-Friction, and the Electricite de France systems are considered. The N00W component of El Centro 1940 earthquake is used as ground excitation. Peak acceleration responses of different secondary systems under various conditions are evaluated and the results are presented as response spectra curves. Particular attention is given to analyzing the effects of mass ratio of the secondary system. The results are compared with the floor response spectra and the significance of the primary-secondary interactions and mass ratio for near tuned conditions are discussed.

BASE ISOLATION SYSTEMS

This section provides brief descriptions of the base isolation systems considered in this study. Laminated Rubber Bearing (LRB) is the most common base isolation system [1,2,18]. This system has been used in a number of structures all around the world including several buildings in California and Utah. A laminated rubber bearing consists of alternating layers of rubber and steel with the rubber being vulcanized to the steel plates. The bearing is rather flexible in the horizontal direction but quite stiff in the vertical direction. The LRB provides protection against earthquakes by shifting the fundamental frequency of vibration to a much lower value and away from the energy containing range of the earthquake ground motion. Figure 1a shows a schematic diagram for the mechanical behavior of the Laminated Rubber Bearing system. This diagram also represents the GERB helical spring and visco-damping base isolation system described in [19].

A Pure-Friction (P-F) isolator offers resistance to motion and dissipates energy only through horizontal friction force [20]. A schematic diagram for the P-F base isolator is shown in Figure 1b. Use of a layer of sand in the foundation of a building which behaves essentially as a Pure-Friction base isolation system was described in [21]. A Resilient-Friction Base Isolation system (R-FBI) is composed of several layers of teflon coated friction plates with a central core of rubber or steel reinforced laminated rubber (Mostaghel and Khodaverdian [22]). The core provides the resilient force for the system, while energy is dissipated by the friction forces. The mechanical behavior of the R-FBI system is illustrated in the schematic diagram shown in Figure 1c. The Alexisismon base isolator of Ikonomou [23] may also be represented by this diagram.

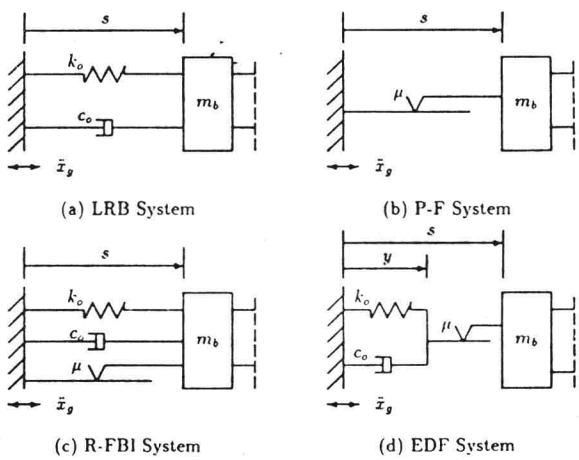

Figure 1. Schematic Diagrams of Isolation Systems

A system which was designed mainly for base isolation of nuclear power plants in regions of high seismicity was developed under the auspices of Electricite de France (EDF) as described in [24]. An EDF base isolator unit consists of a laminated (steel-reinforced) neoprene pad topped by a lead-bronze plate which is in frictional contact with a steel plate anchored to the base raft of the structure. The behavior of the EDF base isolator is shown schematically in Figure 1d.

RESPONSES ANALYSIS

In this study, a three-story building as shown in Figure 2 is used as the primary structure. It is assumed that masses of different floors and the base raft are identical ($m_1 = m_2 = m_3 = m_b = m$) and the stiffness and damping of columns of various stories are also equal. This primary structural model was used earlier in [4,5], and a detail description may be found in these references and in [25]. The secondary system is modeled as a single-degree-of-freedom oscillator with a natural frequency of $f_s = \omega_s/2\pi$ and a damping ratio ζ_s. A value of 0.01 for ζ_s is assumed throughout this study. The values of natural periods T_o ($= 2\pi/\omega_o$), damping ratios ζ_o, and friction coefficients μ for the isolators studied are summarized in Table 1.

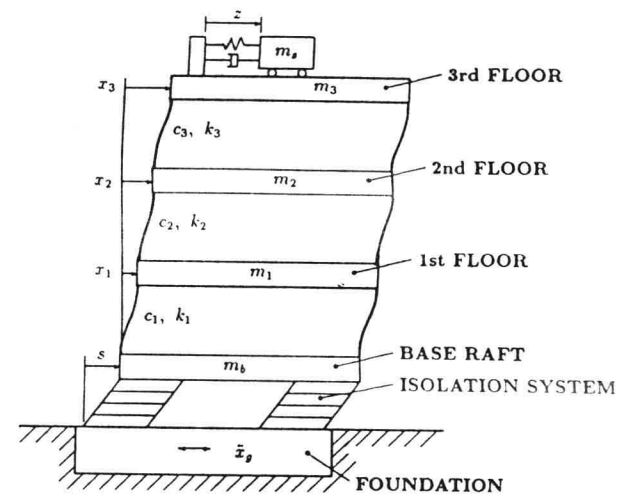

Figure 2. Schematic Diagrams of Primary and Secondary Systems

Base Isolation System	Natural Period T_o (sec)	Damping Ratio ζ_o	Friction Coefficient μ
Larminated Rubber Bearing (LRB)	2	0.08	-
Pure-Friction (P-F)	-	-	0.1
Resilient-Friction (R-FBI)	4	0.08	0.05
Electricite de France (EDF)	1	0.08	0.2

Table 1. Values of Parameters Used for Various Base Isolators

The peak absolute acceleration, $(\ddot{x}_g+\ddot{s}+\ddot{x}_3+\ddot{z})|_{max}$, responses of the secondary system attached to the third floor under a variety of conditions are evaluated. The resulting peak responses presented as acceleration response spectra are discussed in the following sections.

Responses to El Centro Earthquake

The N00W component of the El Centro 1940 earthquake accelerogram is used as the ground acceleration, and peak responses of the secondary system for different base-isolated structures and the fixed-base one are evaluated. A secondary system with a mass ratio ($\gamma = m_s/m_3$) of 0.01 is assumed to be attached to the top floor of the primary structure. The first 20 *sec* of the response time histories are used in these analyses. As noted in [6], the peak response of a secondary system may occur at much later time when compared with the time of peak ground excitation due to the beating phenomenon. To verify that the first 20 *sec* of the response time histories are sufficient for determining the peak responses of secondary systems for El Centro 1940 earthquake, longer time durations for several cases were used. For all the cases studied, peak responses of the secondary system occurred before 20 *sec*.

Figure 3 shows the acceleration response spectra for the secondary system attached to a structure with different base isolation systems. The results for a fixed-base structure are also shown for comparison. It is observed that the acceleration response spectra for the fixed-base structure contains a sharp peak with an amplitude of about $10g$ at the frequency of about 3.33 Hz. This peak is due to tuning of the secondary system to the fundamental frequency of the primary structure. For frequencies more than 5 Hz, the amplitude of the response spectrum vary between 1 to $2g$. Figure 3 shows that the use of base isolation systems eliminates the resonance peak observed for the fixed-base structure, and reduces the peak spectral amplitude by a factor of more than five. The exception is the P-F system which leads to peak acceleration responses comparable to that for the fixed-base structure for the frequency range of $5 < f_s < 12$ Hz.

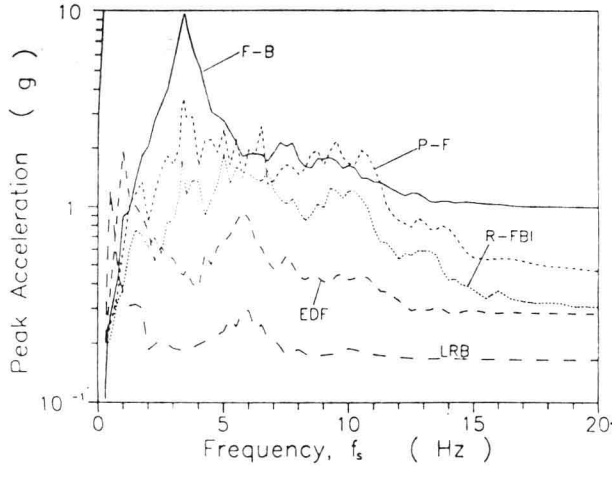

Figure 3. Peak Acceleration Responses of Secondary Systems for El Centro 1940 Earthquake

Figure 3 shows that the trend of variations of peak acceleration of a light secondary system for the R-FBI system is similar to that of the P-F system; however, its magnitude is lower, roughly, by a factor of two. Except for a sharp peak at $f_s \simeq 1$ Hz which corresponds to the natural frequency of the isolator, the spectral amplitude for the EDF system varies between 0.3 to $1g$. It is also noticed that the acceleration spectrum for the LRB system has a peak at $f_s \simeq 0.5$ Hz corresponding to the natural frequency of the bearing used. Away from this peak, the spectral amplitude is about 0.15 to 0.3 g which is the lowest among the isolation systems considered.

Based on the results presented in this section, it may be concluded that, for the El Centro earthquake ground excitation, use of base isolation systems provides considerable protections for the secondary systems and the structural contents. Among the isolators considered, the LRB system leads to the lowest peak acceleration and peak deflection responses in the secondary systems. The frictional systems, however, are less effective in certain high frequency range.

Effects of Mass Ratio

The influences of mass ratio, γ, on acceleration responses of the secondary system are shown in Figure 4. Figure 4a displays the equipment acceleration response spectra for several values of γ for the fixed-base structure. It is observed that for $\gamma = 0.0$, which corresponds to the non-interaction case, the spectrum has a resonance peak at the tuning frequency of $f_s \simeq 3.33$ Hz with an amplitude of about $18g$. Away from this peak, the spectral amplitude decreases rapidly and approaches to zero for small frequencies, and to a value of about $2g$ for large f_s. For $\gamma = 0.001$, it is observed that the acceleration spectrum coincides with that for $\gamma = 0.0$ except for the tuned or near tuned conditions. The peak spectral amplitude for $\gamma = 0.001$ is lower than that for $\gamma = 0.0$ by about $2g$. When γ is increased to a value of 0.01, the response spectrum of the secondary system deviates significantly from the corresponding floor response spectrum for the frequency range near the fundamental frequency of the primary structure. The peak spectral amplitude for $\gamma = 0.01$ is about $10g$. For $8 < f_s < 11$ Hz, small differences between the response spectra for $\gamma = 0.0$ and $\gamma = 0.01$ are also noticed. This is due to tuning of the secondary system to the frequency of the second mode of vibration of the primary structure. Away from these two frequency ranges, the peak acceleration response is identical to that of the non-interaction case. As γ increases to 0.1, it is observed that the peak at $f_s \simeq 3.33$ Hz drops to about $4g$. Furthermore, for large frequencies the peak acceleration experienced by the secondary system becomes slightly larger than the amplitude of the corresponding floor response spectrum.

Figure 4b shows the equipment acceleration response spectra for several values of γ for a structure with the LRB base isolation system. It is observed that the LRB system, generally, leads to low-amplitude acceleration spectra. Furthermore, the spectra for $\gamma = 0.0$, 0.001, and 0.01 are almost identical for the entire range of f_s considered. For $\gamma = 0.1$, the acceleration responses somewhat deviate from those for $\gamma = 0.0$ at $f_s \simeq 0.5$ Hz and $f_s \simeq 6$ Hz. For other frequency ranges, the peak acceleration responses become indistinguishable from the floor response spectra.

The acceleration response spectra for the secondary system for various values of γ in a structure with the P-F system are shown in Figure 4c. It is observed that these spectra contain a number of peaks in the frequency range of 3 to 12 Hz. The peak acceleration response approaches zero for small f_s, and tends to a value of about $0.6g$ for large f_s. For $\gamma = 0.001$, the spectrum is almost identical to that for $\gamma = 0.0$ for the entire range of frequency considered. For $\gamma = 0.01$, certain differences, particularly for the sharp peaks are observed. As γ increases to 0.1, the shape of spectrum becomes quite different from the corresponding floor response spectrum. The interaction between the primary and the secondary system eliminates the sharp peaks, and significantly reduces the amplitude of the response spectrum. For large f_s, the spectral amplitudes for $\gamma = 0.1$ are slightly lower than those for the non-interaction ($\gamma = 0$) case.

Figure 4d shows the peak acceleration responses of the secondary system for several mass ratios for a structure with the R-FBI system. Features of these spectra are similar to those noted for the P-F system. The spectra for $\gamma = 0.0$, 0.001, and 0.01 contain a number of peaks in the frequency range of 3 to 15 Hz, and the interactions between the primary and the secondary systems reduce the spectral amplitudes. For $\gamma = 0.1$, the sharp peaks are eliminated due to the interaction effects. A comparison of Figures 4c and 4d shows that the magnitude of peak acceleration experienced by a non-structural component in a structure with the R-FBI system is much lower than that for the P-F system.

The equipment acceleration response spectra for a structure with the EDF base isolation system are shown in Figure 4e. It is noticed that the spectra contain two sharp peaks, one is at the natural frequency of the isolator ($f_s = 1$ Hz), and the other is at the frequency of about 6 Hz. As mass ratio increases, the magnitude of the maximum acceleration near the sharp peaks decreases. Away from these two peaks, the effects of primary-secondary interactions are relatively insignificant.

The results presented in this section show that, for a secondary system attached to a fixed-base structure, the primary tuning occurs when the natural frequency of the secondary system coincides with the fundamental natural frequency of the structure. While, for a secondary system attached to a structure with a LRB or an EDF base isolation systems, tuning occurs when the natural frequency of the secondary system is close to that of the isolator. For a light secondary system, the effects of primary-secondary interaction are not significant except for the tuned and the near tuned conditions. For mass ratios greater than 1 percent, the interaction effects reduce the peak response of the secondary system for the entire range of frequencies; the amount of reduction are most significant near the tuning frequencies. For frictional systems, such as the P-F and the R-FBI systems, the nature of tuning is not quite clear. The friction force generates high frequency components in the acceleration transmitted to various floors, and the vibration energy is scattered over a broad range of frequencies. The effect of mass ratio in reducing peak responses is similar to those for the fixed-base

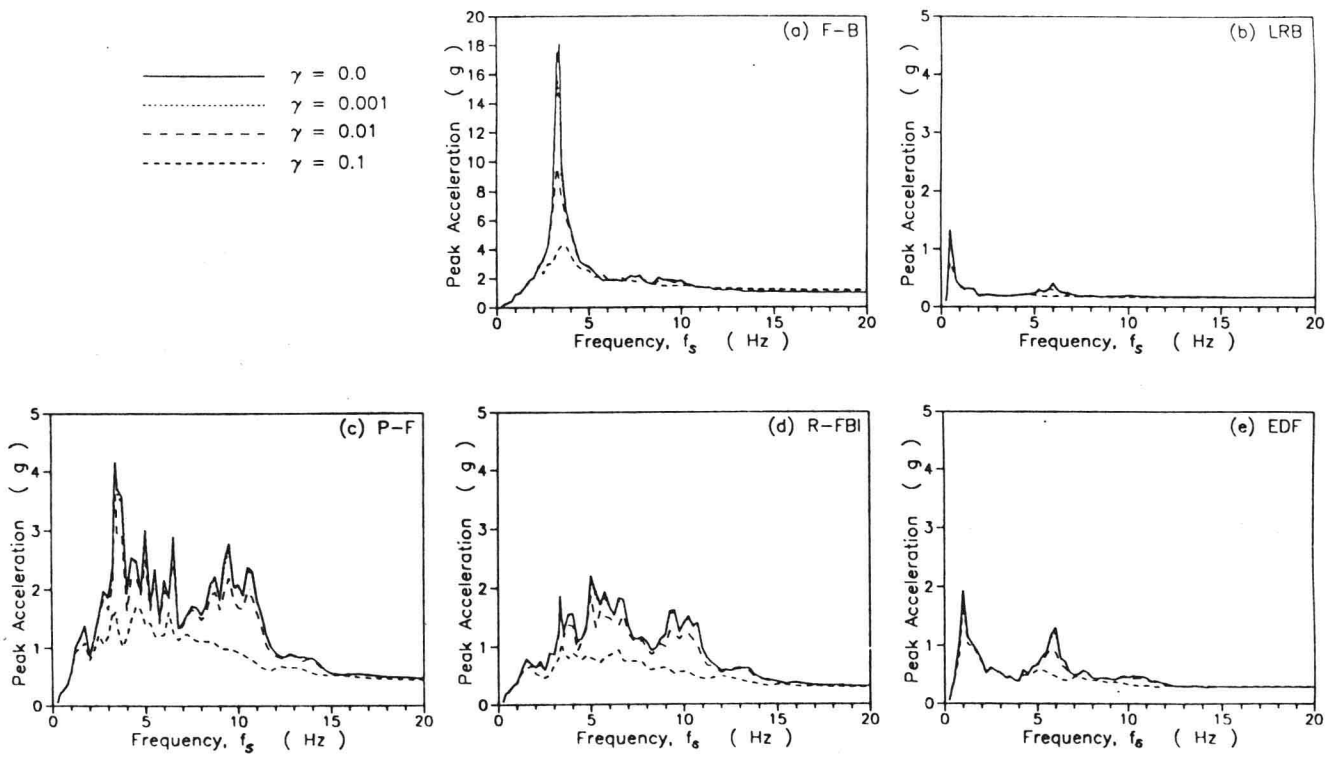

Figure 4. Peak Acceleration Responses of Secondary Systems for Various Mass Ratios for El Centro 1940 Earthquake

structure and the LRB-type base isolators. The results also indicate that the floor response spectra approach, which neglects the primary-secondary interactions, provides conservative estimates for peak responses of equipment and non-structural components.

The effects of damping of secondary systems and the responses to other earthquake ground motions are also studied, and the detail may be found in [25].

CONCLUSION

A study of peak responses of secondary systems attached to a multi-story structure with various base isolation systems under the N00W component of El Centro 1940 earthquake is carried out. The primary-secondary interaction are included in the analysis and the resulting equipment response spectra for different base-isolated structures are compared with those for the fixed-base one under a variety of conditions. Based on the presented results, the following conclusions may be drawn:

1. Peak seismic responses of secondary systems are significantly reduced by using a properly designed base isolation system.

2. Use of base isolation systems eliminates the resonance peaks of the equipment response spectra which occurs at the natural frequency of the fixed-base structure.

3. Mass ratio significantly affects peak responses of secondary systems for the tuned and near tuned conditions.

4. The primary-secondary interactions, generally, reduce the peak response of a secondary system. Thus, the floor response spectra provide conservative estimates for peak responses for tuned or nearly tuned conditions.

5. Among the base isolation systems considered, the linear LRB system leads to the lowest peak responses for secondary systems in most practical cases.

6. The frictional base isolation systems generate high frequency components in the acceleration responses of the structure which could be damaging to siff non-structural components.

In present study, idealized models for various base isolators and structure are used. The nonlinear behavior of rubber at high strain, the velocity dependence of friction coefficient, the soil-structure interaction, and the effect of torsion and rocking of structure are neglected. Nevertheless, the presented results could provide a basis for understanding the behavior of secondary systems in various base-isolated structures. Further refinement of the model to include these additional effects are left for future studies.

ACKNOWLEDGEMENT

This work is supported by the National Center for Earthquake Engineering Research, State University of New York at Buffalo under the Grants No. NCEER 87-2007 and 88-2012A.

REFERENCES

1. Kelly, J.M., *Aseismic Base Isolation: Review and Bibliography, Soil Dyn. Earthquake Engng., 5, pp. 202-216 (1986).*

2. Kelly, J.M., *Aseismic Base Isolation, Shock Vibrat. Dig., 14, pp. 17-25 (1982).*

3. Su, L., Ahmadi, G. and Tadjbakhsh, I.G., *A Comparative Study of Performances of Various Base Isolation Systems Part I: Shear Beam Structures, Earthquake Engng. Struct. Dyn. 18, pp. 11-32 (1989).*

4. Fan, F.-G., Ahmadi, G., and Tadjbakhsh, I.G., *Multi-Story Base-Isolated Buildings Under A Harmonic Ground Motion — Part I. A Comparison of Performances of Various Systems, Part II. Sensitivity Analysis, Nuclear Engng. Design (in press).*

5. Fan, F.-G., Ahmadi, G., Mostaghel, N., and Tadjbakhsh, I.G., *Performance Analysis of Aseismic Base Isolation Systems for a Multi-Story Building, Soil Dyn. Earthquake Engng. (in press), also Report No. MIE-165, Clarkson University, Potsdam, NY, June (1988).*

6. Sackman, J.L., and Kelly, J.M., *Seismic Analysis of Internal Equipment and Components in Structures, Engng. Struct., 1, pp. 179-190 (1979).*

7. Singh, M.P., *Seismic Design Input for Secondary Structure, Journal of Structural Division, ASCE, 106, pp. 505-517 (1980).*

8. Gupta, A.K. and Jaw, J.W., *Coupled Response Spectrum Analysis of Secondary Systems Using Uncoupled Model Properties, Nuclear Engineering and Design, 92, pp. 61-68 (1986).*

9. Igusa, T. and DerKiureghian, A., *Dynamic Characterization of Two-Degree-of-Freedom Equipment Structure Systems, Journal of Engineering Mechanics Division, ASCE, 111, pp. 1-19 (1985).*

10. Kelly, J.M., *The Influence of Base Isolation on the Seismic Response of Light Secondary Equipment, Report No. UCB/EERC-81/117, University of California, Berkeley, CA (1982).*

11. Manolis, G.D., Juhn,G. and Reinhorn, A.M., *Experimental Investigation of Primary-Secondary System Interaction, Report No. NCEER-88-0019, State University of New York at Buffalo, Buffalo, NY, May (1988).*

12. Chen, Y., and Soong, T.T., *STATE-OF-THE-ART REVIEW Seismic Response of Secondary Systems, Engng. Struct., 10, pp. 218-228 (1988).*

13. Kelly, J.M., *The Influence of Base Isolation on the Seismic Response of Light Secondary Equipment, Repot No. EPRI-NP-2919, Electric Power Research Institute, Palo Alto, CA, (1983).*

14. Kelly, J.M., and Tsai, H.C., *Seismic Response of Light Internal Equipment in Base-Isolated Structures, Earthquake Engng. Struct. Dyn., 13, pp. 711-732 (1985).*

15. Ikonomou, A.S., *Parasitic Response of Equipment in Base Isolated Structure Mounted on Sliding Bearing*, in *Seismic Engineering, Recent Advances in Design, Analysis, Testing and Qualification Methods, PVP-Vol 127, ASME, pp. 405-411 (1987).*

16. Wu, T. and Seidensticker, R.W., *Sensitivity Studies of a Seismically Isolated system to Low Frequency Amplification, in Seismic Engineering, Recent Advances in Design, Analysis, Testing and Qualification Methods, PVP-Vol. 127, ASME, pp. 461-467 (1987).*

17. Fan, F.-G. and Ahmadi, G., *Floor Response Spectra for*

Base-Isolated Multi-Story Structures, Earthquake Engng. Struct. Dyn. (in press), also Report No. MIE-177, Clarkson University, February (1989).

18. Kelly, J.M., and Hodder, S.B., *Experimental Study of Lead and Elastomeric Dampers for Base Isolation Systems in Laminated Neopreme Bearings, Bulletin of New Zealand National Society for Earthquake Engng., 15, pp. 53-67 (1982).*
19. Huffmann, G.R., *Full Base Isolation for Earthquake Protection by Helical Springs and viscodampers, Nuclear Engng. Design, 84, pp. 331-338 (1985).*
20. Mostaghel, N. and Tanbakuchi, J., *Response of Sliding Structures to Earthquake Support Motion, Earthquake Engng. Struct. Dyn., 11, pp. 729-748 (1983).*
21. Li, L., *Base Isolation Measure For Aseismic Building in China, Proc. 8WCEE, San Francisco, CA, July 21–28, Vol.VI, pp. 791-798 (1984).*
22. Mostaghel, N. and Khodaverdian, M., *Dynamics of Resilient-Friction Base Isolator (R-FBI), Earthquake Engng. Struct. Dyn. 15, pp. 379-390 (1987).*
23. Ikonomou, A.S., *Alexisismon Seismic Isolation for Translational and Rotational Seismic Input, Proc. 8WCEE, San Francisco, CA, July 21-28, Vol.V, pp. 975-982 (1984).*
24. Gueraud, R., Noel-Leroux, J.-P., Livolant, M., and Michalopoulos, A.P., *Seismic Isolation Using Sliding-Elastomer Bearing Pads, Nuclear. Engng. and Design, 84, pp. 363–377, (1985).*
25. Fan, F.-G. and Ahmadi, G.,*Seismic Responses of Secondary Systems in Base-Isolated Structures, Rept. No. MIE-187, Clarkson University, June 1989.*

ELASTOMERIC BEARINGS FOR THREE-DIMENSIONAL SEISMIC ISOLATION*

F. F. Tajirian
Bechtel National Incorporated
San Francisco, California

J. M. Kelly and I. D. Aiken
University of California
Berkeley, California

W. Veljovich
Rockwell International
Canoga Park, California

ABSTRACT

Seismic isolation offers an attractive approach for reducing seismic loads in nuclear structures, and more significantly, in reactor components. In this paper a novel isolation system which can be used in certain low rise buildings to isolate horizontal and vertical ground motions is proposed. It consists of steel-laminated elastomeric bearings which provide flexibility in both the horizontal and vertical directions by using thick rubber layers bonded to steel shim plates. An extensive testing program of scaled bearings was carried, and in general it was confirmed that it would be feasible to use such bearings to isolate stiff buildings with low center of gravity in both the horizontal and vertical directions.

INTRODUCTION

In recent years, several systems for seismic isolation of buildings have been proposed and implemented [Kelly, 1986]. Today there are over 125 structures worldwide which are isolated and the numbers have been increasing steadily in the last few years. This is especially true in Japan, where since 1982, over 20 seismically isolated buildings have been constructed [Kelly, 1988], and another 16 have received construction permits [Kitagawa, 1989]. The majority of these systems use steel-laminated elastomeric bearings to isolate the building and its contents from the horizontal components of the earthquake ground movement. Elastomeric bearings can be designed to provide a wide range of vertical stiffness and horizontal stiffness. In general elastomeric bearings have been designed to be very stiff in the vertical direction such that the vertical components of the earthquake are transmitted through the foundation to the structure relatively unchanged.

In certain cases a double isolation system has been used where the building is isolated in the horizontal direction and only equipment that are sensitive to vertical motions are isolated locally in the vertical direction. An example of this approach is the High Technology Research Laboratory building in Tsukuba Japan, which is isolated in the horizontal direction using steel laminated elastomeric bearings and steel bar dampers, and air springs are used to isolate an electron microscope in the vertical direction [Ohbayashi Corp., 1988]. The effectiveness of this design both in isolation of ambient vibrations as well as seismic motions has been demonstrated. A similar approach has been proposed in the conceptual design of a large 1500 MWe liquid metal fast breeder reactor (LMFBR), the Superphenix 2 in France. The entire nuclear island is isolated in the horizontal direction using elastomeric pads and viscous dampers, and additionally, the reactor cavity is isolated in the vertical direction using helical steel springs and viscous dampers [Feuillade and Richard, 1986].

Systems which are flexible in the horizontal as well as in the vertical direction have also been proposed for three-dimensional (3-D) isolation of buildings. One such system, which consists of large blocks of unreinforced natural rubber, was used to isolate a school building in Skopje, Yugoslavia [Siegenthaler, 1970]. Although additional development work was carried out on this system including shake table tests [Staudacher, 1984], it has not been implemented in other buildings. Another proposed system for 3-D seismic isolation of buildings uses large steel helical springs and viscodampers commonly used for vibration isolation of large machine foundations [Huffmann, 1985]. In both these systems, the vertical stiffness is close to the horizontal stiffness. Thus when they are used to isolate buildings the horizontal and rocking response will be coupled resulting in large vertical accelerations at the corners of the building even in the presence of input which is purely horizontal and the possibility of liftoff of the isolators.

For buildings of low aspect ratio (height to width ratio less than two), and with a low center of gravity, the concept of (3-D) isolation becomes practical as the concern for overturning and uplifting can be considerably lessened. This concept can be especially useful for buildings or structures which house equipment that are sensitive to vertical motion

* Work performed under the auspices of U.S. Department of Energy, under Contract No. DE-03-88SF17468

such as electronic equipment and some nuclear reactor components. In this paper, a novel isolation system which can be used for 3-D isolation of such buildings is proposed. It uses steel-laminated elastomeric bearings with thick layers of rubber that provide flexibility in the horizontal direction and some flexibility in the vertical direction. These bearings have the added advantage that they would isolate the building and contents from ambient ground vibrations, and they could be more easily removed for inspection by cmpressing the bearing.

A design using this approach was developed for an Advanced Liquid Metal Reactor (LMR) building concept, the Sodium Advanced Fast Reactor (SAFR). SAFR was supported by the U.S. Department of Energy (DOE) and was being developed by a team led by Rockwell International. Support for this program was terminated in 1989.

A series of tests were performed on prototype quarter-scale SAFR bearings at the Earthquake Engineering Research Center (EERC) of the University of California in Richmond, California to examine the feasibility of using the proposed bearings for 3-D isolation of nuclear buildings, and to verify the applicability of existing design formulas. The results and main conclusions of the testing program are summarized below.

Description Of The SAFR Design

SAFR employs a 450 MWe pool type LMR as its basic module. The reactor assembly module is a standardized shop-fabricated unit housed in a building constructed above grade with plan dimensions of 124 ft. by 82 ft. [Oldenkamp et al., 1988] as shown in Figure 1. The total weight of the reactor building and its contents is 63,000 kips. Seismic isolation was incorporated in the SAFR reference design to support plant standardization, enhance plant safety margins, permit siting in zones with higher seismicity, and potentially reduce plant costs.

The building is supported on 100 steel-laminated elastomeric bearings which provide both horizontal and vertical isolation. The design horizontal frequency is 0.5 Hz and the vertical frequency is 3 Hz. The low vertical frequency is achieved by using bearings with thicker rubber layers bonded to fewer steel shims. Such bearings are referred to as low shape factor (LSF) bearings where the shape factor, S, is defined as the compressive area divided by the area free to bulge for a single layer. For circular bearings S becomes,

$$S = \frac{D'}{4t}$$

where D' is the steel shim diameter and t is the thickness of a single rubber layer.

To date, interest in low shape factor (LSF) bearings has been mainly for the development of isolation systems that can isolate buildings from horizontal earthquake loading as well as ambient ground vibrations (horizontal plus vertical). In Japan, Kajima Corporation has demonstrated the effectiveness of such systems by constructing an acoustic laboratory on LSF bearings [Koshida et al., 1989] with a horizontal frequency of 0.5 Hz and a vertical frequency of 5 Hz. Analysis, vibration testing, and recorded earthquake data have demonstrated the advantages of this system.

The SAFR bearings have a diameter of 42 in., a total height of 16.25 in., and consist of three layers of rubber each 4 in. thick separated by two 1/8 in. steel shims resulting in a shape factor of 2.3. In contrast, elastomeric bearings which are stiff vertically have shape factors which exceed 15. The required design bearing horizontal and vertical stiffnesses are 16.1 kip/in and 580 kip/in, respectively.

The seismic design basis is a design safe shutdown earthquake (SSE) with a maximum horizontal and vertical acceleration of 0.3 g anchored to a design earthquake that envelopes the NRC Regulatory Guide 1.60 spectra. The selected criteria are expected to cover over 80 percent of potential nuclear sites in the U.S. excluding California. Options for siting in higher seismic zones, with design earthquakes exceeding 0.5 g, were investigated and were found acceptable.

Results Of Seismic Analysis

Dynamic analyses were performed to compare the response of SAFR with and without isolation. A comparison of horizontal and vertical response spectra at the reactor supports is shown in Figure 2. It can be seen that there are substantial reductions in horizontal accelerations at all the equipment resonant frequencies. In the vertical direction, the response is amplified at the vertical isolation frequencies, but is reduced at frequencies greater than 4 Hz which is the range of equipment vertical frequencies. The maximum SSE horizontal displacement of the bearings was computed to be 9 in. In general, a large amount of rocking will result in buildings supported on such bearings. However, because of the low center of gravity of the SAFR building and its wide base only a small amount of uplift due to rocking was computed in the corner bearings.

Seismic Isolator Tests

It was recognized from the onset of this program that bearing tests would have to be performed to demonstrate the feasibility of using LSF bearings and to verify the validity of design equations. An extensive experimental program was undertaken at EERC to investigate the performance characteristics of the the SAFR LSF bearings. The test series had the following objectives:

- Evaluation of vertical stiffness
- Evaluation of horizontal stiffness and damping, and the influence of vertical load on these characteristics
- Identification of failure modes under axial load and combined axial and shear
- Investigation of the effect of end plate connection on the performance and stability of bearings under extreme loads.

Six quarter-scale bearings were tested (see Table 1 for dimensions). Two types of bearing to foundation connections were considered: a dowel type connection, and a rigidly bolted type connection (see Figure 3). Additionally, two types of natural rubber compound: a filled (high-damping) rubber and a conventional unfilled rubber were investigated.

A total of 265 nondestructive tests were performed on the bearings followed by failure tests. Each bearing was tested individually in the test fixture shown in Figure 4. The fixture is capable of applying horizontal displacements of ±6 in. at a maximum velocity of 30.0 in/sec or 10 in. in any one direction. In this paper, due to space limitations, only the results for the unfilled rubber bearings are presented. The high damping bearing results will be reported elsewhere. The bolted bearing will be referred to as LB and the dowelled as LD.

TEST RESULTS

Vertical Tests

A series of vertical tests were performed in which each bearing was loaded monotonically from zero load to peak loads of 15.9, 31.8, 47.7, and 63.6 kips and back to zero load. The cyclic vertical stiffness around an initial vertical load, which is more relevant from the design point of view, was also measured for four initial axial load levels and are shown superimposed on the 63.6 kips monotonic test in Figure 5. The vertical stiffness was observed to increase with increasing vertical load, however, at a much smaller rate than was observed for previously tested high shape factor bearings [Kelly et al., 1990]. The ratio of cyclic to monotonic stiffness for the four axial load levels was computed. For the design level load (7 percent axial prestrain), there is about a 15 percent increase in vertical stiffness. The full-scale vertical stiffness based on extrapolation of measured values at the design vertical load is 588 kip/in which compares well with the design target value of 580 kip/in.

The effect of horizontal displacement offset on cyclic vertical stiffness was also examined. In general there was a slight increase in stiffness with increasing strain level. For example, the increase in vertical stiffness between zero offset and 1.5 in. offset (50 percent shear strain) was only 5 percent.

The equivalent viscous damping coefficient was evaluated from the vertical hysteresis loops and was found to exceed 17 percent for the unfilled rubber compound. The damping was essentially independent of the horizontal offset and amplitude of the applied vertical load. The measured damping exceeds the damping used in the analysis which was limited to 10 percent. A comparison of bolted and dowelled bearing results showed that the end plate connection detail had no influence on the vertical stiffness and damping.

Horizontal Tests

A series of tests were performed in which each bearing was subjected to five cycles of horizontal load at 0.75 Hz to constant values of peak shear strain ranging from 10 to 160 percent while maintaining a constant vertical load. Four levels of axial load were applied, 15.9, 31.8, 47.7, and 63.6 kips. The hysteresis loops for the design axial load of 31.8 kips for the LD bearing are superimposed for different strain levels in Figure 6 and the loops at 160 percent strain for the four axial load levels are superimposed in Figure 7. The horizontal stiffness as a function of shear strain for different axial load levels is shown in Figure 8. It can be seen that the horizontal stiffness is high at low strains and decreases at higher strains but is fairly constant above 40 percent strain. Additionally, the bolted bearing horizontal stiffness is not sensitive to vertical load. This is in contrast to the results obtained from the dowelled bearings, where the stiffness was observed to be highly sensitive to vertical load.

The equivalent viscous damping ratio in the horizontal direction for the design level axial load and 50 percent shear strain the damping was computed to be about 5.5 percent. The damping was observed to be more sensitive than horizontal stiffness to axial loads and increased significantly at higher axial loads especially for the dowelled bearings. This type of behavior has also been observed in tests of bearings with high shape factors which showed that as the applied axial load tended to the bearing buckling load, the damping of the bearing increased [Koh and Kelly, 1987].

Shear Failure Tests

A series of large shear strain tests were performed on the bolted and dowelled bearings. The objective of these tests was to fail a bearing in shear while subjected to a constant vertical load. An initial loading cycle of 50 percent strain was performed to determine the stiffness of the bearings prior to any degradation. The axial load during these tests was 31.8 kips. Subsequently the bolted bearings were deformed horizontally to maximum strains corresponding to 200, 225, 328, and 344 percent. The force displacement plots for these tests are shown in Figure 9. A photograph of the bearing at 330 percent strain is shown in Figure 10. The first evidence of failure was seen during the 328 percent strain test, where, at approximately 9.5 in. (320 percent strain) a change in stiffness was observed. This coincided with tearing of the bottom elastomer layer. It should be noted that the subsequent 344 percent strain test revealed only a small loss of stiffness beyond about 4 in. of displacement, and even though the bearing was failed in the previous test, it was capable of accommodating loads in excess of that at which significant damage to the bearing had first occurred. In fact, after the bearing had totally failed and it was forced back to its original position, it showed no signs of distress when the 50 percent test was repeated. This finding implies that current acceptance test specifications which require that bearings be tested up to 100 percent shear under the design axial load will not be capable of detecting potential defects in the bearings. Thus as part of acceptance tests, it would be important to shear the bearings under the minimum axial load possible.

Another important observation is that as previously observed in high shape factor bearing tests [Tajirian et al., 1990], the horizontal stiffness of bolted bearings increases appreciably at shear strains greater than 150 percent thus providing an inherent mechanism for limiting displacements during extreme events.

Large displacement shear tests were also performed on the dowelled bearing to investigate geometric instability or roll-out. These tests were performed for various axial load levels and peak strain levels of 100, 200, and 263 percent, and ending with repetition of the 100 percent test. Figure 9-b shows the force-displacement relationship for an axial load of 31.8 kips. Roll-out (disengagement of the dowels) occurred in this case around 7 to 7.5 in. or about 250 percent strain. As can be seen in Figure 11 that even after the initiation of roll-out, the bearing continues to provide resistance. This is partly due to the fact that the bearing is flexible in the horizontal direction, and it tends to roll in the available confined space. The test was repeated for an axial load of 15.9 kips and roll-out once again occurred at around 7 in. The 50 percent tests performed prior to and following both roll-out tests showed that there was negligible loss of stiffness even after the bearing and its internal plates underwent extreme shape distortions. The stiffening effects observed in the bolted tests were not as pronounced in these tests.

The extrapolation of these results to full-scale bearings show that they would be capable of accommodating 38 in. of horizontal displacement in the bolted configuration and 28 in. in the dowelled configuration. This means that there would be a margin of 4 for the design earthquake of 0.3 g for the bolted case, and a margin of 3.1 for the dowelled case.

Loading Frequency Effects

Tests to investigate the effects of loading frequency on the bearing stiffness and damping were performed for hori-

zontal and vertical loading conditions. In general, it was observed that rate effects were small and that variations due to other factors masked any rate-related trends.

Tension Failure Tests

Pure tensile tests were performed on a high-damping bolted bearing to determine the uplift capability of LSF bearings. The first set of tests consisted of full cycles of tension-compression loading at increasing amplitudes. The axial load-vertical displacement plots for these tests are shown overlain in Figure 11. As to be expected there is a noticeable difference between the tensile and compressive stiffness. While the tensile stiffness corresponds to the tensile stiffness of the elastomer, the compression stiffness is influenced by additional factors such as the shape factor.

The remaining tests consisted of half-cycles of tensile load applied until failure was induced. The tensile load vertical displacement plots are shown in Figure 12. The highest load reached was 31.4 kips. Visible tearing of the top rubber layer of the bearing was observed during the later stages of this loading cycle. However, even with initiation of failure, subsequent tests showed that the bearings were capable of sustaining a peak tensile load of 22 kips. The ultimate tensile stress based on the shim plan dimensions was about 500 psi.

CONCLUSIONS

Dynamic tests performed on reduced scale low shape factor (LSF) steel-laminated elastomeric bearings confirmed the feasibility of using such bearings for horizontal and vertical seismic isolation of certain types of buildings such as the SAFR LMR power plant building. The tests demonstrated that it is possible to design bearings that have the necessary horizontal and vertical stiffness to achieve 3-D isolation. Furthermore, the bearings are capable of accommodating extreme horizontal displacements with margins four times the displacements computed for the SSE level earthquake. Bolted bearings are preferable to dowelled connections because they can accommodate larger horizontal displacements and remain stable even under very low axial loads. Furthermore, the vertical and horizontal stiffness for such a configuration is independent of the axial load in the range of the applicable design load. Additionally, the horizontal stiffness of bolted bearings increases substantially at high shear strain levels providing an inherent mechanism for limiting displacements during extreme events. Tensile tests demonstrated the capability of bolted bearings in providing resistance against uplift. No damage or degradation of bearing mechanical properties was observed even after several cycles of extreme loading which resulted in severe distortions of the bearing geometries. To further proof this design, it would be necessary to perform tests on larger scale bearings, as well as shake table experiments to verify system response. Finally when using bolted bearings it is essential to demonstrate that high quality bearings can be manufactured where ultimate failure always occurs due to rupture of the elastomer and not bond failure.

REFERENCES

Feuillade, G., and Richard, P., 1986, "Evolutions des Dispositifs Parasismique du Batiment Reacteur du Projet SPX2 Depuis 1980 et Consequences Sur les Chargement du Bloc Reacteur," *1er Colloque National de Genie Parasismique*, St-Remy-Les-Chevreuse, France.

Huffmann, G. K., 1985, "Full Base Isolation for Earthquake Protection by Helical Springs and Visco-dampers," *Nuclear Engineering and Design,* Vol. 84, No. 3.

Kelly, J. M., 1986, "Aseismic Base Isolation: Review and Bibliography," *Soil Dynamics and Earthquake Engineering*, Vol. 5, No. 3.

Kelly, J. M., 1988, "Base Isolation in Japan, 1988," *Report No. UCB/EERC-88/20,* Earthquake Engineering Research Center, University of California, Berkeley, CA.

Kelly, J. M., Aiken, I. D., and Tajirian, F. F., 1990, "Mechanics of High Shape Factor Elastomeric Seismic Isolation Bearings," *Report No. UCB/EERC-90/ 01*, University of California, Berkeley, CA.

Kitagawa, Y., 1989, "Base-Isolated Building Structures in Japan," *5 Jomadas Chilenas de Sismologia e Ingenieria Antisismica*, Chile.

Koh, G. C. and Kelly, J. M., 1987, "Effects of Axial Load on Elastomeric Isolation Bearings," *Report No. UCB/EERC-86/12,* University of California, Berkeley, CA.

Koshida, H., et al, 1989, " Vibration Tests and Earthquake Observation Results of Base-Isolated Building," *Seismic, Shock, and Vibration Isolation,* ASME PVP-Vol. 181.

Ohbayashi Corporation, 1988, "Ohbayashi Base Isolation System and Base Isolated Buildings," Technical Report.

Oldenkamp, R. D., Brunings, J. E., Guenther, E., and Hren, R., 1988, "Update-Sodium Fast Reactor (SAFR) Concept," *Proc. of American Power Conference*, Vol. 50.

Seigenthaler, R., 1970, "Earthquake-Proof Building Supporting Structure with Shock Absorbing Damping Elements," *Schweizerische Bauzeitung*, Nr. 20.

Staudacher, K., 1984, "Structural Integrity in Extreme Earthquakes, The Swiss Full Base Isolation System," *8th World Conference in Earthq. Engin.,* San Francisco, CA.

Tajirian, F. F., Kelly, J. M., and Aiken, I. D., 1990, "Seismic Isolation for Advanced Nuclear Power Stations," *Earthquake Speectra,* EERI, May.

Table 1 Comparison of SAFR Bearing Properties

	Full Scale	Quarter Scale
Outside diameter (in.)	42	10
Thickness of end plates (in.)	2	1
Number of rubber layers	3	3
Thickness of rubber layers (in.)	4	1
Number of steel shim plates	2	2
Thickness of shim plates (in.)	0.125	0.105
Diameter of shim plate (in.)	38	9
Total bearing height (in.)	16.25	5.21
Shape Factor	2.4	2.3
Design vertical load (kips)	630	31.8
Design pressure (psi)	455	405

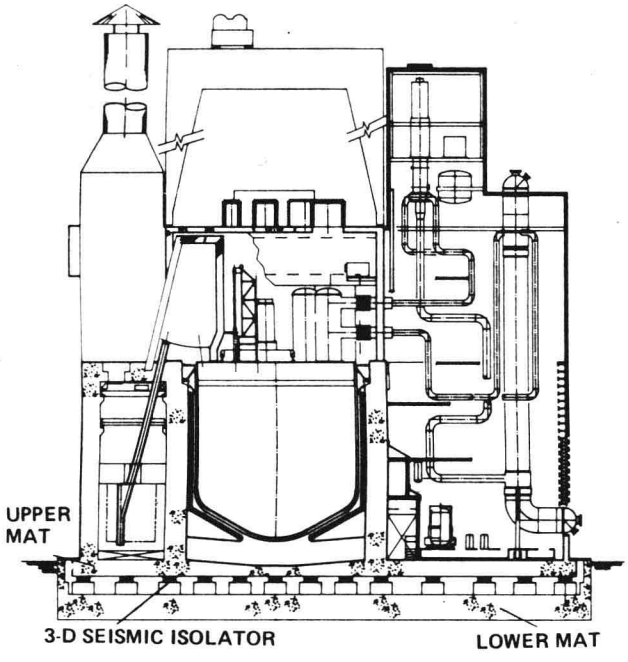

Fig. 1 Section of SAFR Plant

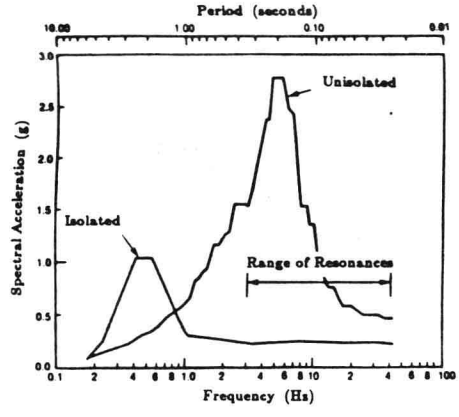

(a) Horizontal Direction

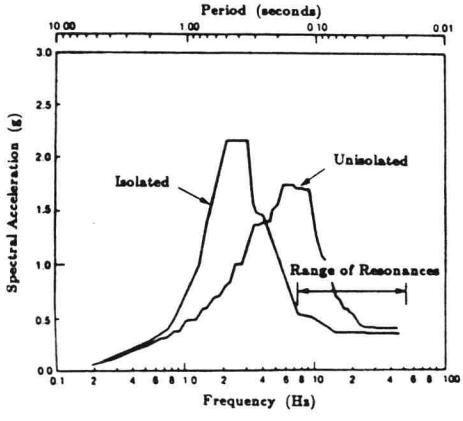

(b) Vertical Direction

Fig. 2 Comparison of SAFR Response Spectra

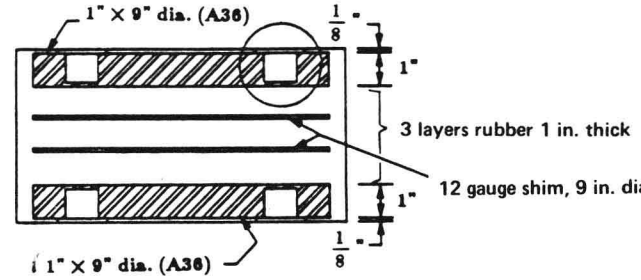

(a) Dowelled (LD) Bearing

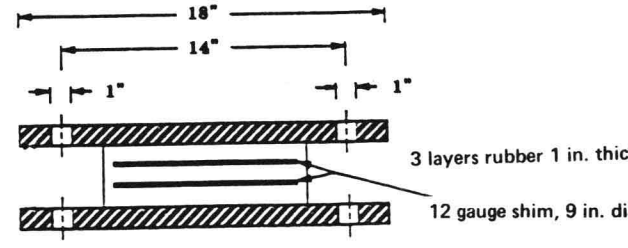

(b) Bolted (LB) Bearing

Fig. 3 Typical Quarter-Scale LSF Bearing

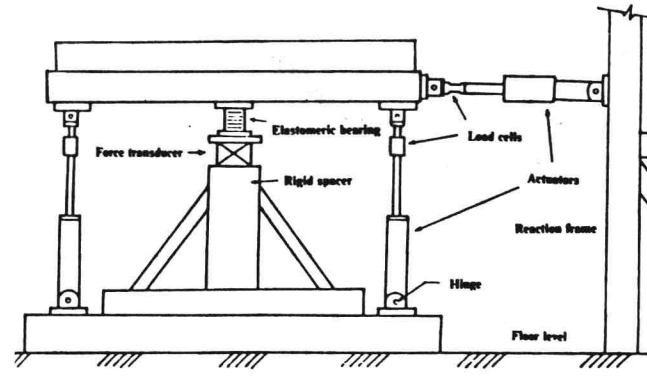

Fig. 4 EERC Single Bearing Test Machine

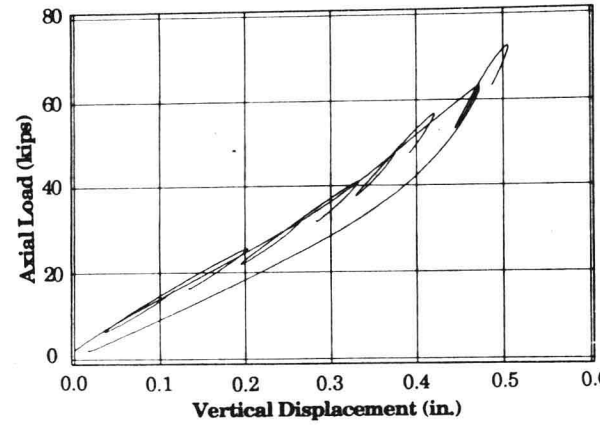

Fig. 5 Cyclic Vertical Loading Superimposed on Monotonic Vertical Loop for Axial Load = 61 kip, LB Bearing

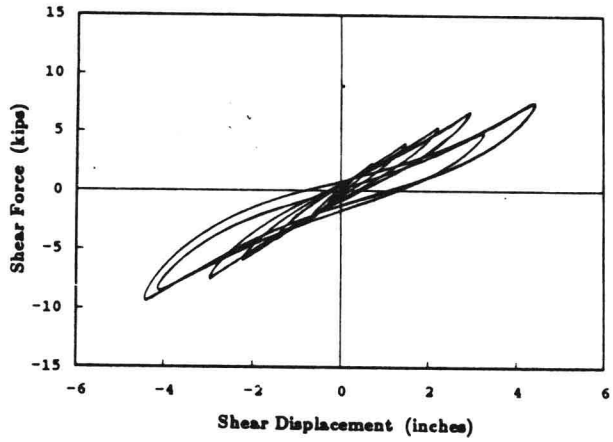

(a) LD Bearing

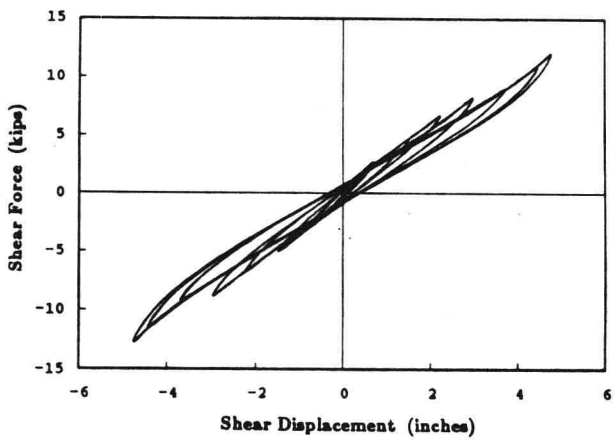

(b) LB Bearing

Fig. 6 Hysteresis Loops for Cyclic Shear Tests, Constant Axial Load = 31.8 kips

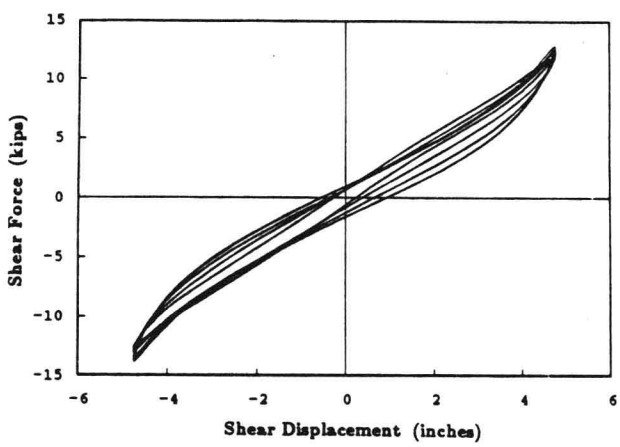

Fig. 7 Hysteresis Loops for Cyclic Shear Tests, Four Axial Loads, Constant 160% Shear Strain

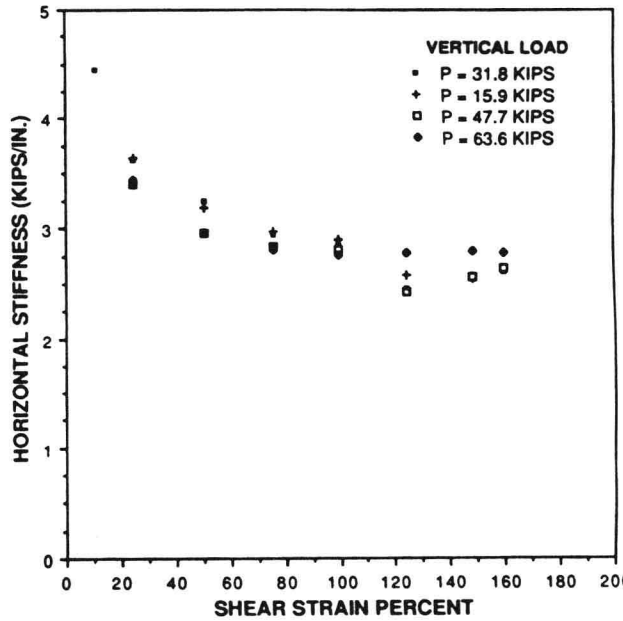

Fig. 8 Effective Horizontal Stiffness vs. Shear Strain, LB Bearing

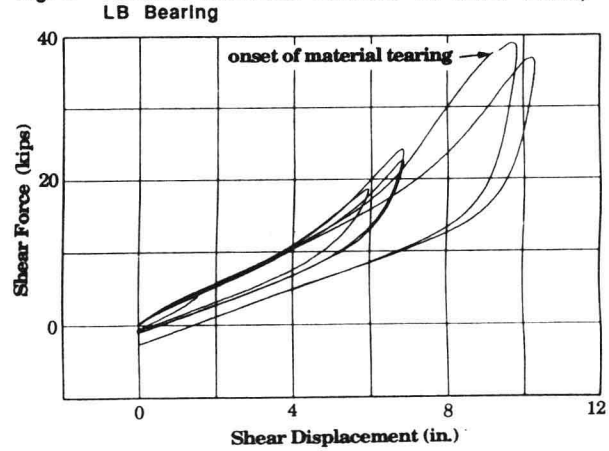

(a) LB Bearing

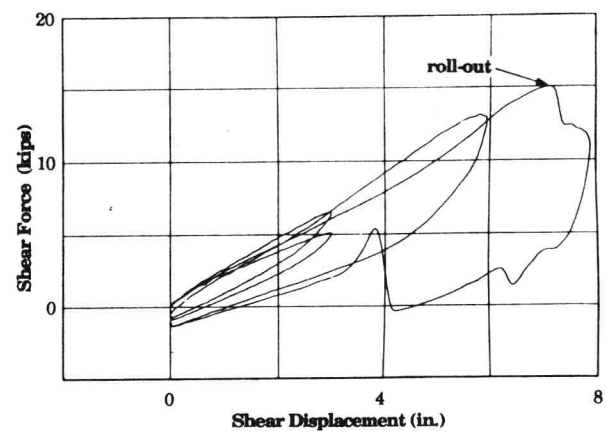

(b) LD Bearing

Fig. 9 Shear Force vs. Horizontal Displacement, Failure Test, Constant Axial Load = 31.8 kips